SLAC-PUB-372
September 1967

NUCLEON FORM FACTORS ABOVE 6 GeV*

R. E. Taylor

Paper delivered at the International Symposium on Electron and Photon Interactions at High Energies, Stanford Linear Accelerator Center, September 1967.

---

*Work supported by U. S. Atomic Energy Commission.

NUCLEON FORM FACTORS ABOVE 6 GeV

R. E. Taylor
Stanford Linear Accelerator Center
Stanford University, Stanford, California

I. INTRODUCTION

This report describes the results from a preliminary analysis of an elastic electron-proton scattering experiment, performed at the Stanford Linear Accelerator Center. The experiment is being carried out by a collaboration of physicists from SLAC, Cal Tech, and M.I.T.*

The preceding paper by G. Weber has summarized the data on proton form factors obtained from other accelerators at momentum transfers squared (q^2) up to 10 $(GeV/c)^2$. We have measured cross sections for e-p scattering in the range of q^2 from 0.7 to 25.0 $(GeV/c)^2$, providing a large region of overlap with previous measurements. In this experiment we measure the cross section by observing electrons scattered from a beam passing through a liquid hydrogen target. The scattered particles are momentum analyzed by a magnetic spectrometer and identified as electrons in a total absorption shower counter.

Data have been obtained with primary electron energies from 4.0 to 17.8 GeV and at scattering angles from 12.5 to 35.0 degrees. In general, only one measurement of a cross section has been made at each momentum transfer. In these circumstances, separation of the electric and magnetic form factors (G_E and G_M) cannot be made from our data. However, since the relation $G_E = G_M/\mu$ has been shown to hold at low momentum transfers and the contribution of G_E to the cross section falls off rapidly with increasing q^2, we are able to indicate the behavior of the magnetic form factor at high momentum transfers.

II. THE EXPERIMENTAL EQUIPMENT

A general layout of the beam line from the accelerator to the target area (end station A) is shown in Fig. 1. The primary electron beam is momentum analyzed and transported to the target by a magneto-optic system in the beam switchyard. A simplified drawing of this system is shown in Fig. 2. The beam is collimated and passed through the first bending magnet (BM1) and then through momentum defining slits (S). Quadrupoles image the collimator on the slits. The slits may be adjusted to define a momentum pass band ($\Delta p/p$) in the range 0.1 - 2.5%, and the transmitted beam is then focussed onto the target. The focussing is achromatic.

The momentum spread of the beam used in the experiment was generally less than 0.5% to maintain kinematic separation between the elastic peak and inelastic cross section varies rapidly with energy. Extensive magnetic measurements and

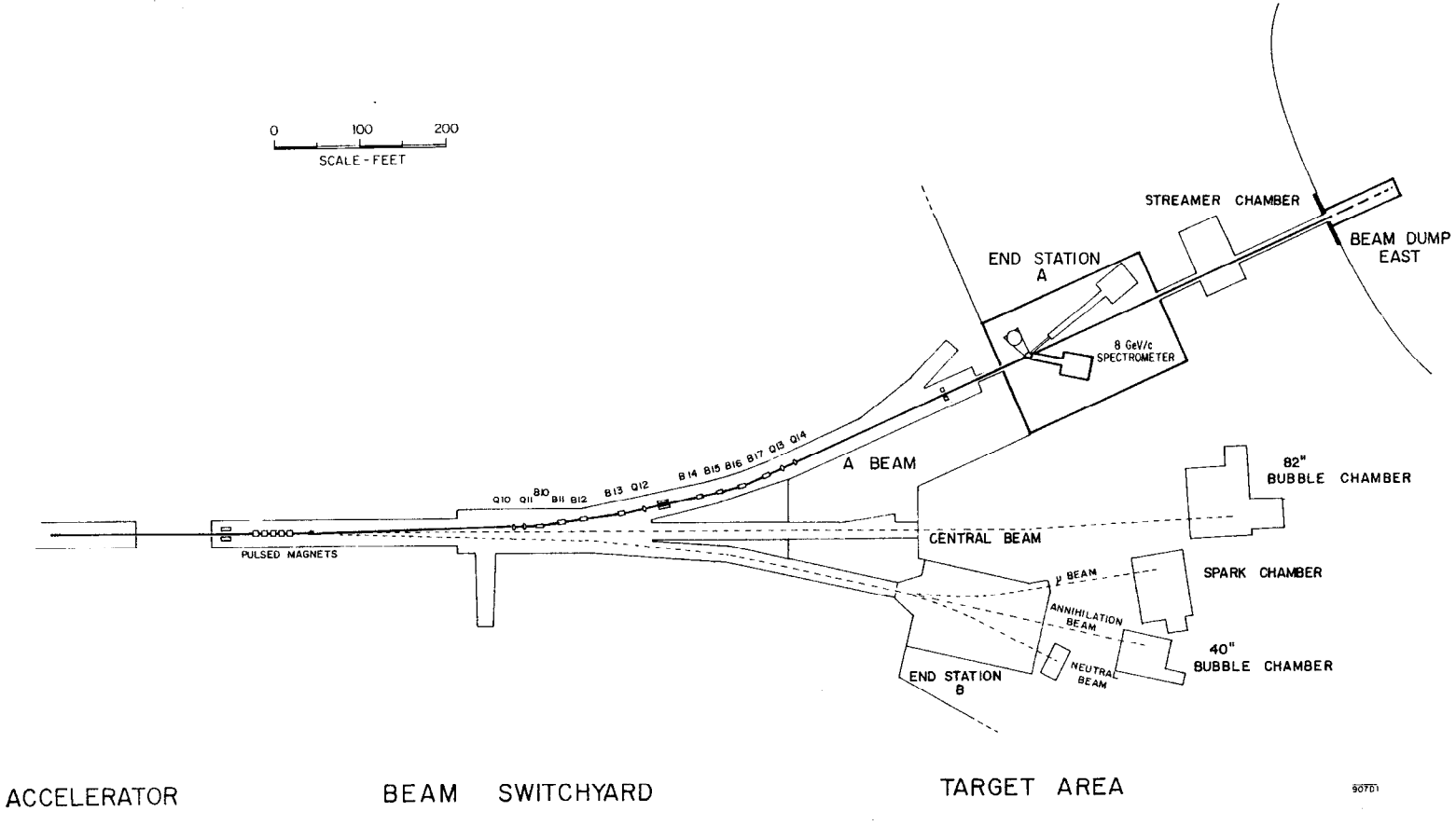

FIG. 1 --General layout of the beam line from the accelerator to the target area in end Station A.

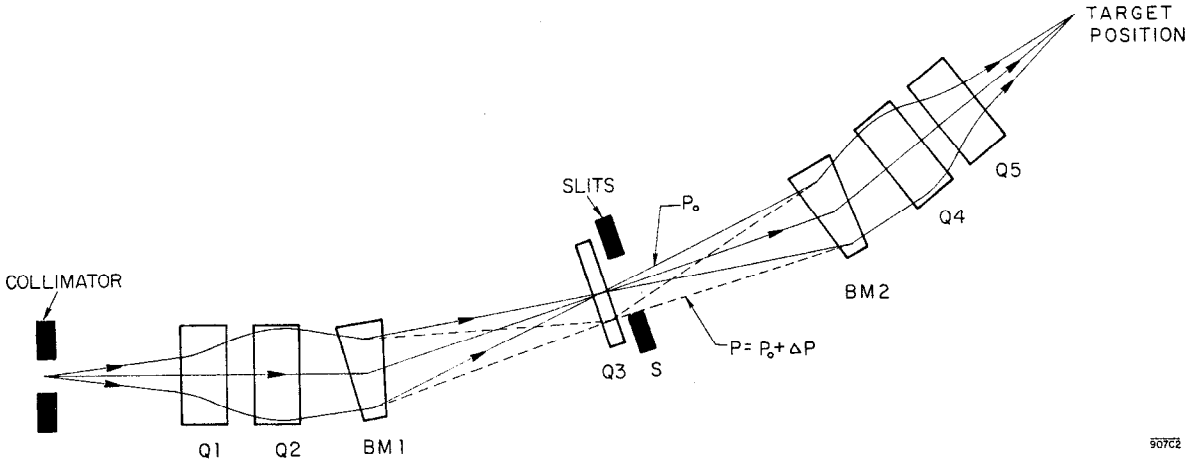

FIG. 2 --A simplified drawing of the switchyard beam optics, in which the emittance is independent of the initial momentum bite.

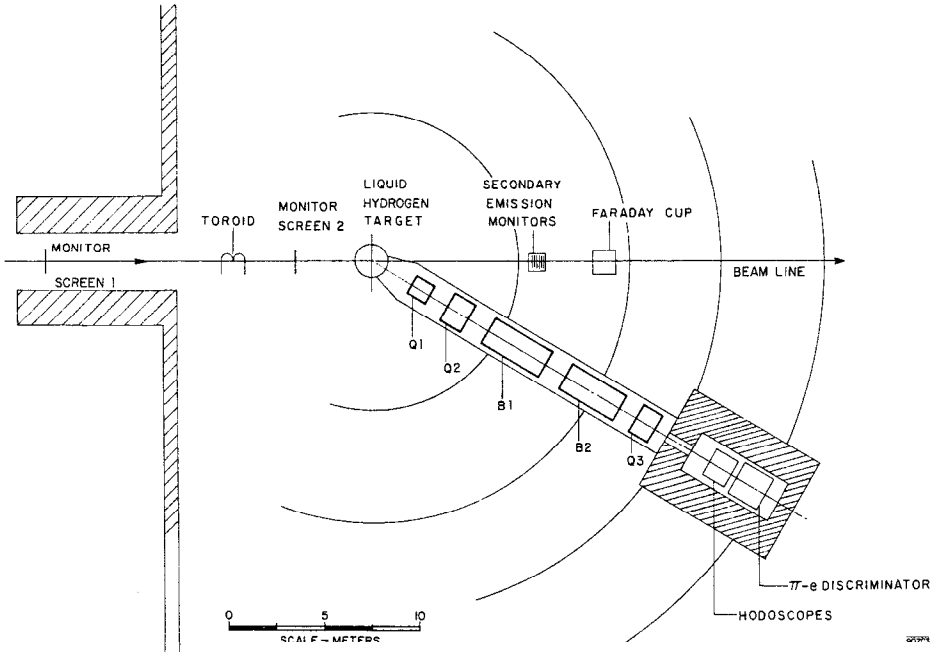

precision surveying allow this energy to be fixed to better than 0.5%. This uncertainty introduces less than 3% error in our cross sections.

The analyzed beam emerges into the larger of the two SLAC end stations through a heavy shielding wall (as in Fig. 1). By adjusting upstream steering coils and monitoring the position of the beam on two fluorescent screens one can align and position the beam at the target to within about 1 mm. This defines the direction of the incident beam to better than 0.1 mr. To minimize backgrounds arising from the disposal of the beam during data runs, the beam is taken through the end station to the beam dump located approximately two hundred feet behind the target area.

A plan view of the equipment near the target is shown in Fig. 3. The incident electron beam current is monitored using a toroid-transformer and two thin-foil secondary emission monitors. The Faraday cup[1], is used for regular intercalibrations of the monitors, and can be remotely removed from the beam line during data runs.

Electrons which scatter from the liquid hydrogen target are momentum analyzed using the SLAC 8 GeV/c magnetic spectrometer.[2] The spectrometer consists of two bending magnets (B1 and B2), three quadrupoles (Q1 - 3), and detectors (hodoscopes and a π-e discriminator, which includes a total absorption shower counter) mounted on a rigid frame which can be rotated about a vertical axis passing through the target. An elevation view is seen in Fig. 4. A heavy concrete and iron shield surrounds the detectors and is supported separately from the frame holding the magnets and detectors.

The design parameters of the spectrometer are listed in Table I, and the spectrometer optics are illustrated in Fig. 5. The vertical (momentum dispersing) plane has point-to-point focussing, and a detector hodoscope at the p-focal plane defines the momentum ($\Delta p/p$) to $\pm$ 0.05%. Parallel-to-point focussing in the horizontal plane allows the use of a long target, and a hodoscope defines the scattering angle (θ) to $\pm$ 0.15 mr in the θ-focal plane. We require this precision in the angular information because the momentum of elastically scattered particles varies with the scattering angle by much more than a momentum resolution width over the angular acceptance of the spectrometer. An astigmatic focus serves to separate the p and θ foci by 0.5 m, so that the detector hodoscopes may be conveniently located. The momentum focal plane is tipped forward at an angle of 14° to the central ray by chromatic aberrations in the quadrupoles. The accelerator beam was used to trace out orbits in the spectrometer, and the results were in good agreement with computer calculations. Figure 6 shows the calculated and measured acceptance apertures of the spectrometer for particles from the center of the target with the spectrometer set to the momentum of the incident electron beam.

Figure 7 shows a simplified schematic of the detector system. Two arrays of scintillation counters are used to locate a particle in the p- and θ-focal planes. The θ-array has 55 overlapping counters covering an angular range of 16 mr, and the p-array has 41 overlapping counters covering a total of 4% in $\Delta p/p$. These arrays are bracketed by trigger counters. The rest of the detector system in Fig. 7 are elements of an elaborate π-e discriminator. Particle identification in this experiment was made using only the total absorption shower counter. The requirement of a reasonable pulse-height in this counter reduced background events

TABLE I

The Design Parameters of the 8 GeV/c Spectrometer

Maximum Momentum	8.5 GeV/c
Horizontal Beam Position Acceptance	± 10 cm
Horizontal Angle (θ) Acceptance	± 7.8 mr
θ Dispersion	4.405 ± 0.010 cm/mr
Vertical Angle (Φ) Acceptance	± 29.5 mr
Solid Angle	0.75 mster
Momentum (p) Acceptance	± 2.0%
p Dispersion	2.92 ± 0.10 cm/%
Tilt of p-Focal Plane	14.2° ± 0.6°
Length from Target to θ-Focal Plane	21.50 m
Separation Between p- and θ-Focal Planes	0.50 m

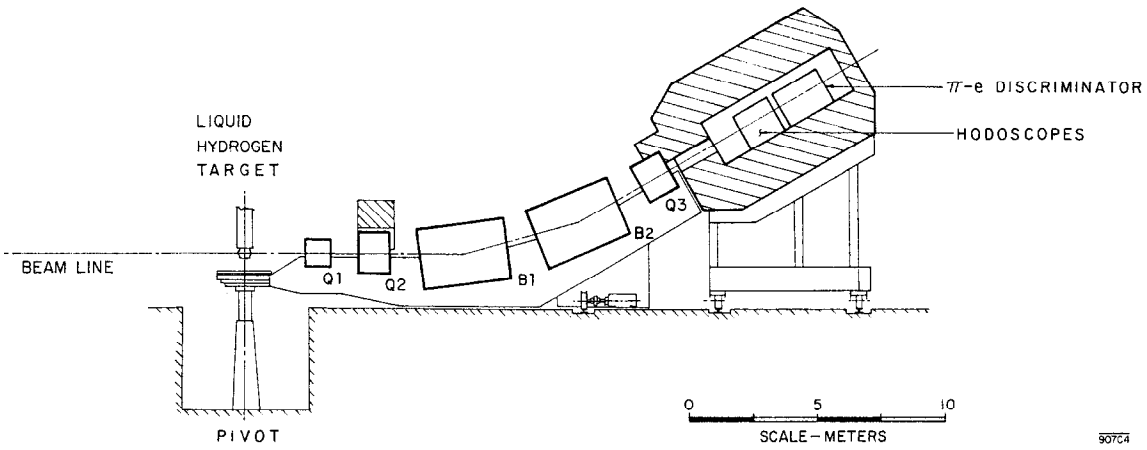

FIG. 4 --Elevation view of the SLAC 8 GeV/c magnetic spectrometer.

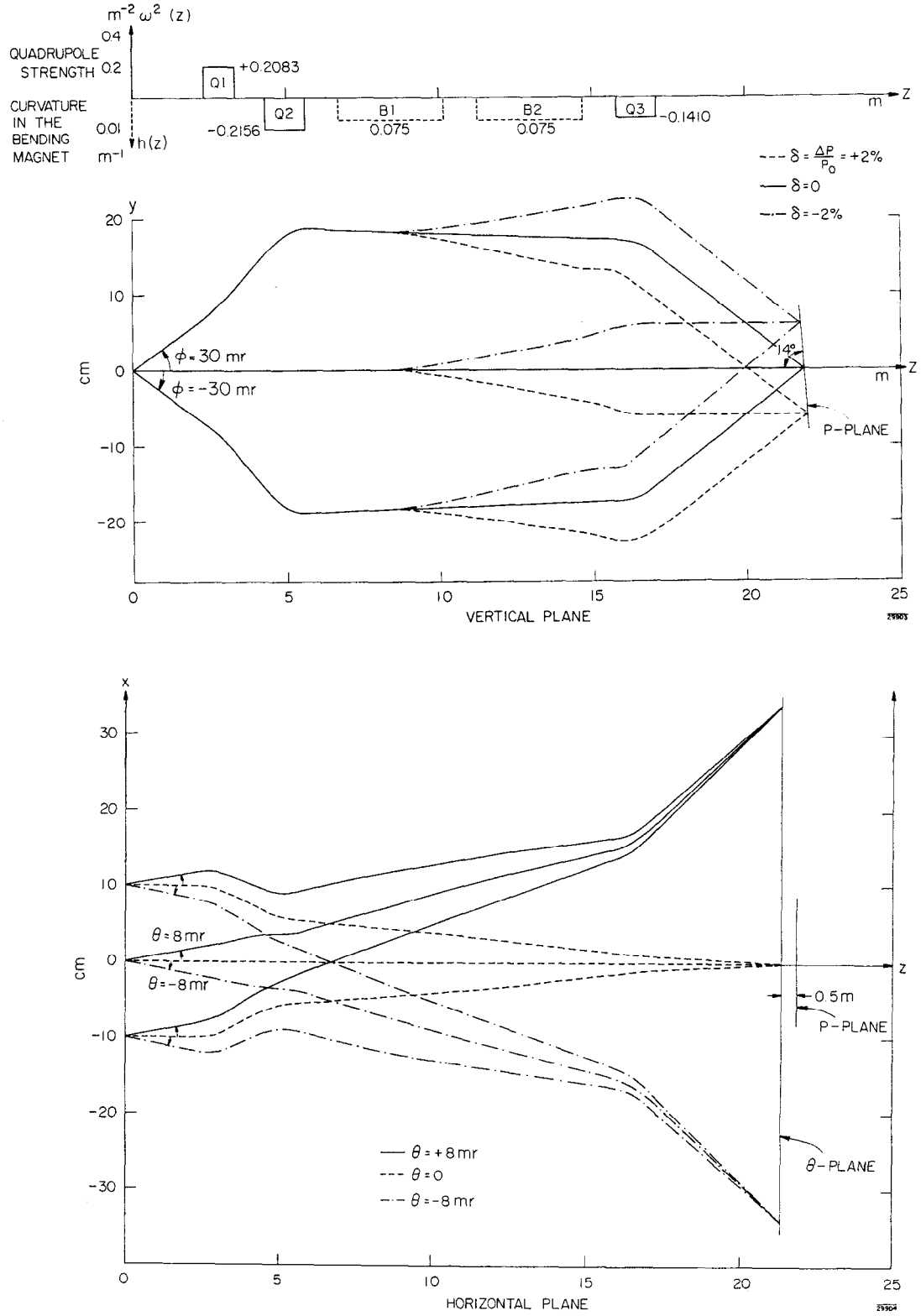

FIG. 5 --The 8 GeV/c spectrometer optics for the vertical and horizontal planes.

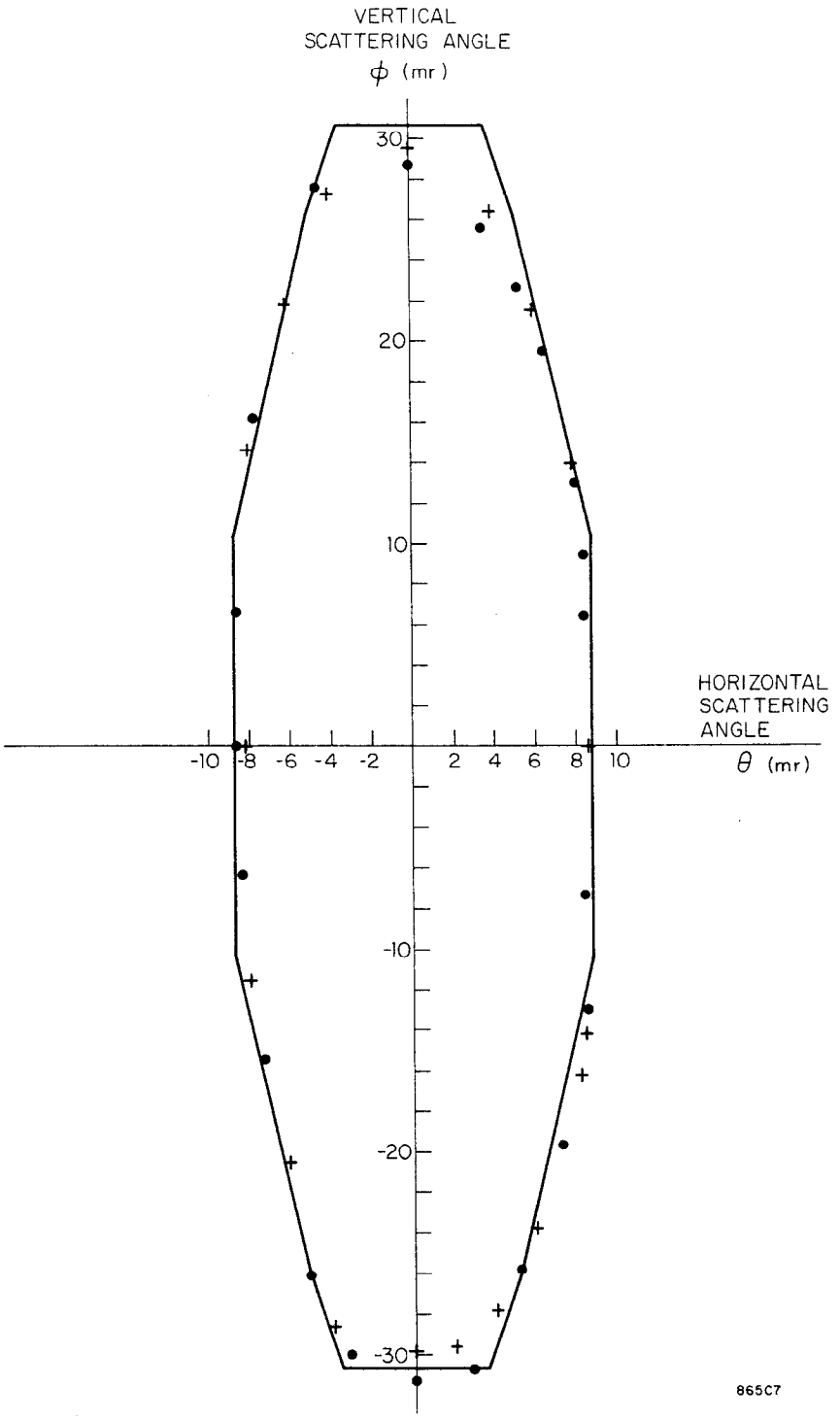

FIG. 6 --The acceptance aperture of the 8 GeV/c spectrometer for electrons from the center of the target and with the spectrometer set to the momentum of the incident beam. The points indicate the measurements using two beam energies (● = 8 GeV, + = 6 GeV). The solid line is the acceptance aperture from computer calculations.

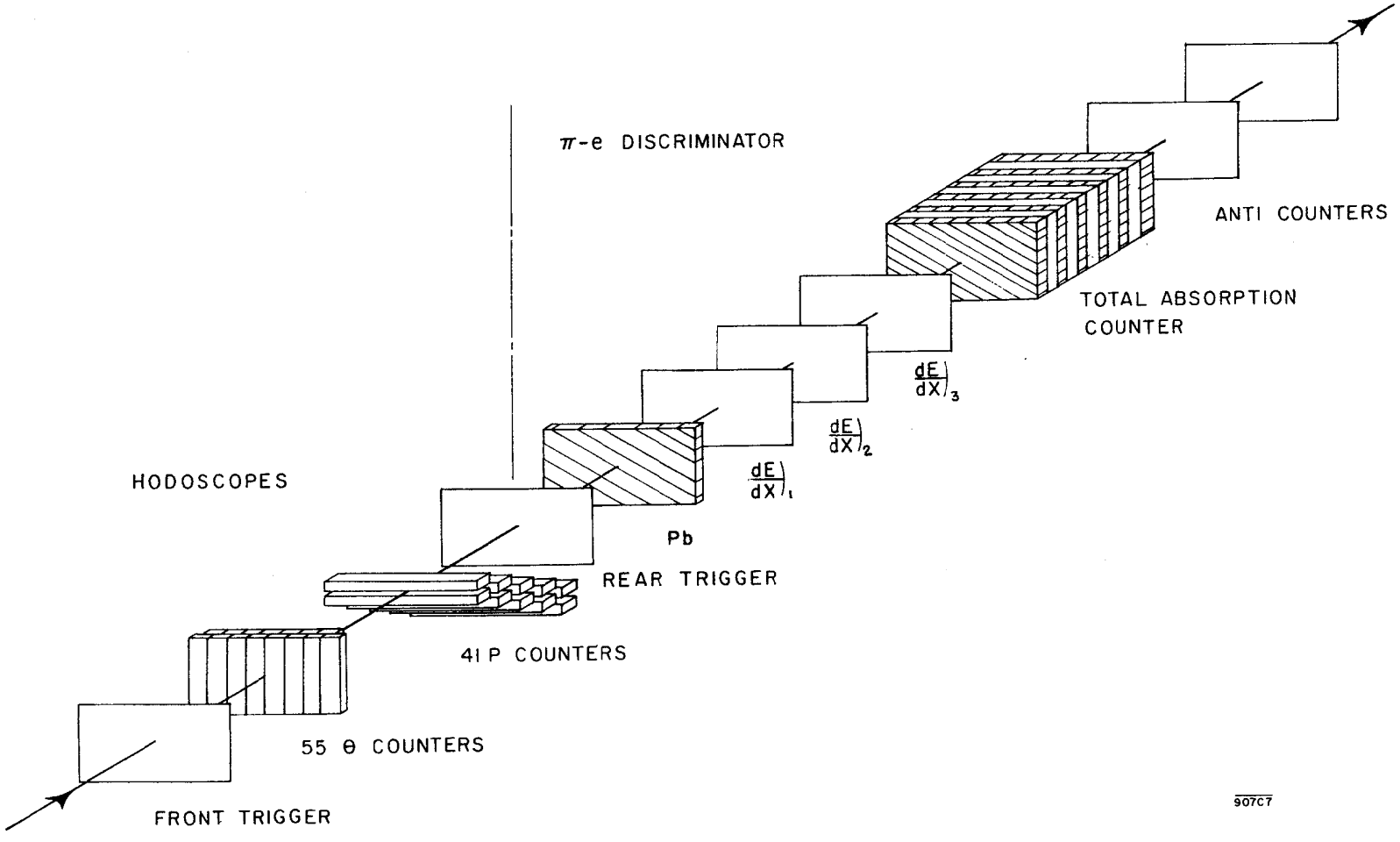

FIG. 7 --A schematic of the detector system used with the 8 GeV/c spectrometer

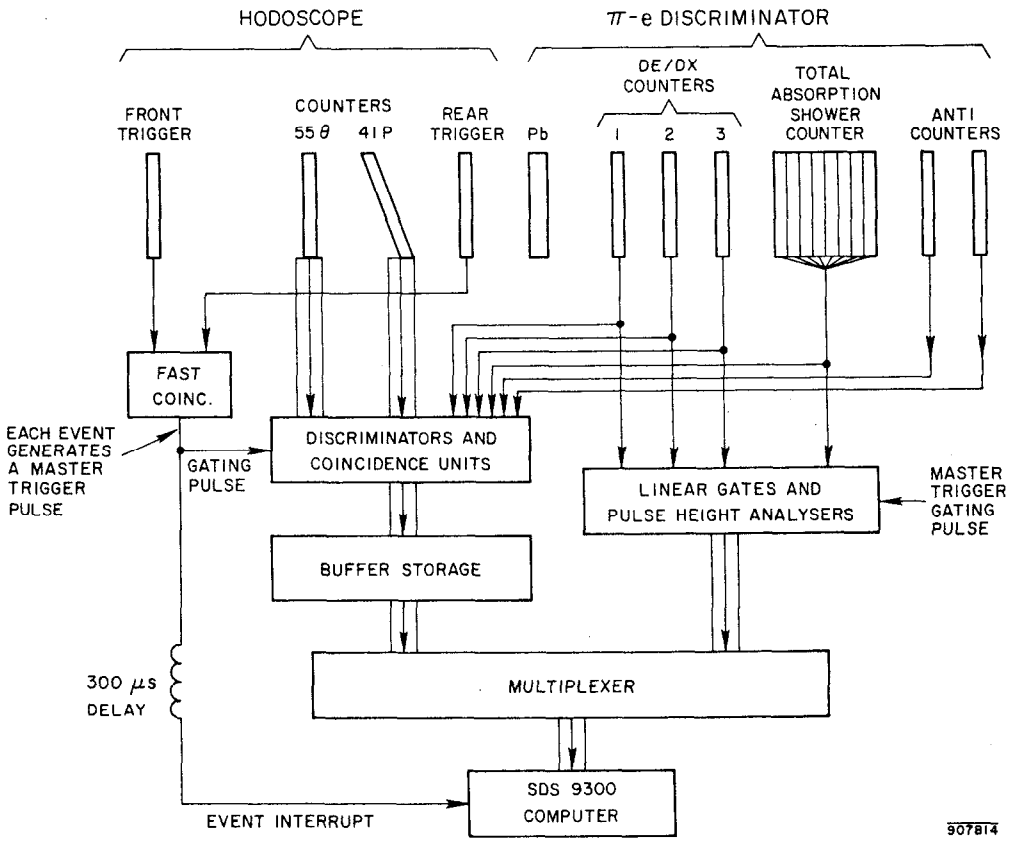

FIG. 8 --A simplified block diagram of the detector logic system.

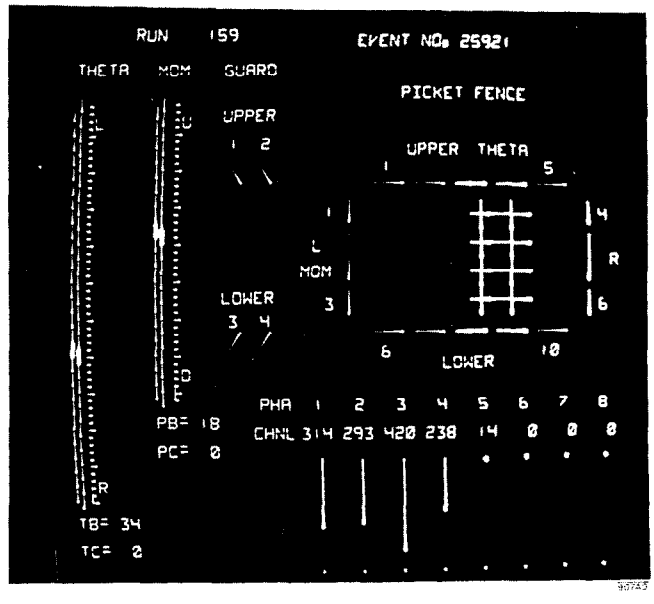

FIG. 9 --This figure is the first of a series to illustrate the kind of information provided by the on-line computer. A scope display of a single event is shown. Explanation of the patterns is given in the text.

in the hodoscopes to levels below the statistical accuracy of our measurements. Additional information, such as from three dE/dx counters and anti-counters, is available, but has not been used in the analysis of the experiment to date.

Data recording, diagnostics, and control of a large fraction of the experimental equipment is performed on-line using an SDS-9300 digital computer, which is large enough to provide extensive on-line analysis of the data. A simplified diagram of the detector logic is given in Fig. 8. A fast coincidence between the trigger counters defines an "event" and generates a "master trigger" which gates the discriminated outputs of each counter in the hodoscopes into temporary buffer storage and initiates pulse height analysis of the dE/dx and total absorption counters. The "master trigger" also generates an interrupt signal to the computer to allow it to accept the data stored in temporary storage. An "event" requires twelve 24-bit words of computer storage which contain coded information such as the state of all the momentum, angle and anti-counters, pulse-heights in the dE/dx and total absorption counters and miscellaneous singles and coincidence conditions applying to the event. The computer writes blocks of events onto magnetic tape and, as time permits, samples the incoming events for on-line analysis. The on-line analysis is comparable in scope to the final off-line analysis, and together with a powerful set of display programs for the scope, provides a thorough monitoring of the data and the equipment.

For a data run at a given spectrometer angle, the computer sets the spectrometer magnets to the expected momentum of the elastically scattered electrons. As an event is sampled on-line, the values of p and θ are calculated from the hodoscope counters which fired. The missing mass of the recoil particle is then calculated assuming a two-body reaction. For elastic scattering this mass should correspond to the mass of the proton. Resolution and radiative effects smear out the observed peak.

Illustrating the kind of information available from the computer, Fig. 9 shows the scope display for a single event. The grids to the left of the figure indicate the scintillation counters in the θ-array ("theta") and p-array ("mom"). The path of the scattered electron is shown by the intense spots, which indicate two overlapping adjacent counters in each array. The "picket fence" is from a coarse hodoscope in the π-e discriminator which has not been used in this experiment. The pulse heights in each of the dE/dx counters and in the total absorption counter are indicated both as channel numbers and by lines of length proportional to pulse height in the lower right of the figure.

Figure 10 is a pulse height spectrum for the total absorption counter. This data is from a run at $q^2 = 2.5$ $(GeV/c)^2$ where the total number of events is given at the top of the figure (14,049), and the peak in the spectrum corresponds to electrons of 8 GeV/c. If we demand that all "good events" (electrons) have a pulse height greater than channel 100 in this counter we will suppress most of the pions and other background particles and yet lose only a negligible fraction of events from the electron shower. The p-θ plane distribution for these "good events" is shown in Fig. 11, where 11,542 events satisfied the pulse height requirement. The angle counters are displayed along the x-axis and the momentum along the y-axis. Due to kinematics the elastic peak lies along a line which is tilted with respect to the p-counters. The elastic peak and radiative tail are clearly seen. There are a few events in the upper half of the plane which are kinematically

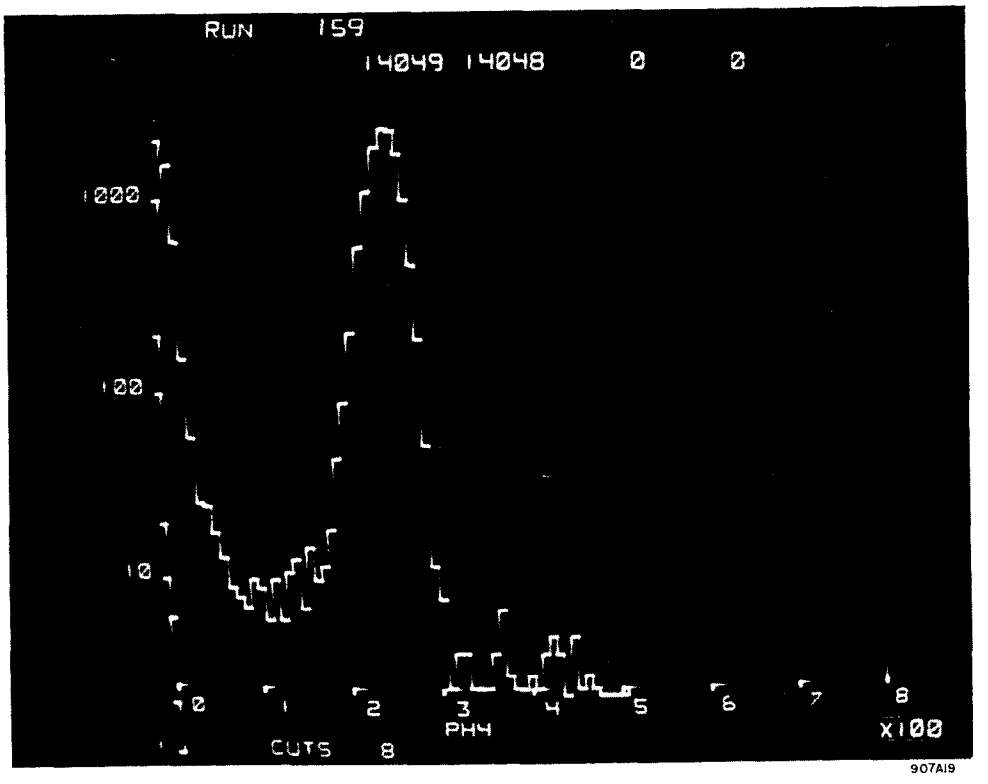

FIG. 10 --A pulse height spectrum of the total absorption shower counter. The peak corresponds to 8 GeV/c electrons.

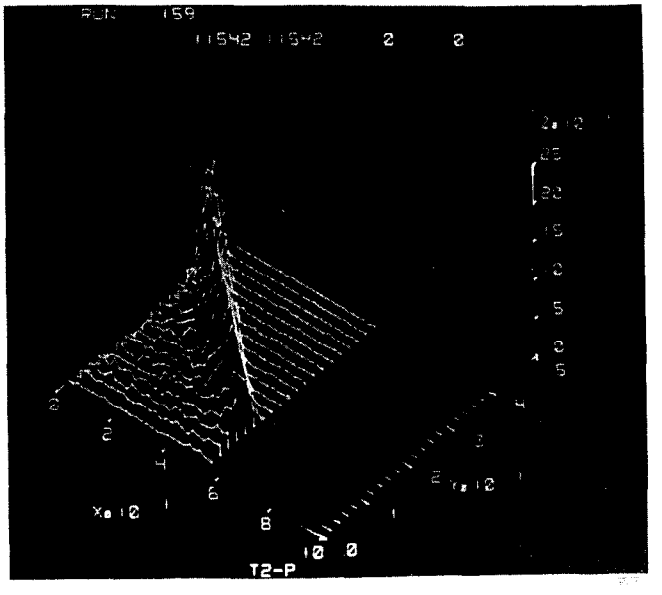

FIG. 11 --A distribution of "good events" in the p-θ plane for a run at $q^2 = 2.5$ (GeV/c)^2. The θ-counters are displayed along the x-axis and the p-counters along the y-axis. The elastic peak and radiative tail are clearly seen.

forbidden for elastic scattering from the proton, and these can be subtracted out with "target empty" runs. For each event in Fig. 11 the missing mass is calculated and the distribution is displayed, as in Fig. 12. The missing mass plot shows the customary shape of an elastic peak with a radiative tail towards higher missing masses (lower scattered electron energy). The elastic peak occurs at 970 rather than at 938 MeV because of 0.5% difference in momentum calibration between the spectrometer and the beam switchyard. (In our analysis, we have assumed that the switchyard value of momentum is correct.)

All displays can also be obtained on the line printer. Figure 13 shows a missing massing plot in this display mode.

The effectiveness of the discrimination between electrons and background particles is illustrated in Fig. 14, where the distribution of events as a function both of total absorption counter pulse height (x-axis) and missing mass (y-axis) is shown. The elastic electron peak clearly stands out from the unwanted background which does not have the typical "elastic" shape in missing mass.

III. EXPERIMENTAL RESULTS

In selecting the data points we were limited to a maximum primary electron energy (E) of 18 GeV during this period of machine running. Another restriction is the limit of closest approach of the 8 GeV/c spectrometer to the beam, which corresponds to a data point scattering angle (θ) of about 12 degrees. Figure 15 shows the points in the E $-\theta$ plane where we have taken data. The limits of maximum E and minimum θ are shown as broken lines in the figure, and the solid lines indicate the values of E and θ for constant scattered momenta (P) and constant four momentum transfers squared (q^2). Most of the data have been taken at a maximum counting rate consistent with these constraints. The cross sections measured vary from around 10^{-31} cm^2/ster at the lowest q^2 point to 2×10^{-39} cm^2/ster at the highest q^2.

Cross sections were calculated from the following relation

$$\frac{d\sigma}{d\Omega} = \frac{N_{pk} C}{N_e N_p \Delta\Omega} \qquad (1)$$

where

N_{pk} is the number of events in the region of the elastic peak from the missing mass spectra (Fig.12). Subtractions for target windows have been made either by runs on a dummy target, or by scaling the number of events above the kinematic limit into the region of the elastic peak.

N_e is the number of incident electrons measured by the transformer-toroid, which is regularly calibrated against the Faraday cup.

N_p is the number of protons/cm^2 for each of the three targets used (14.7, 27.6, and 31.7 cm). The density of liquid hydrogen was taken as 0.07035 gm/cm^3 corresponding to the temperature and pressure of the target cell in our design. No correction has been made for bubbling in the target.

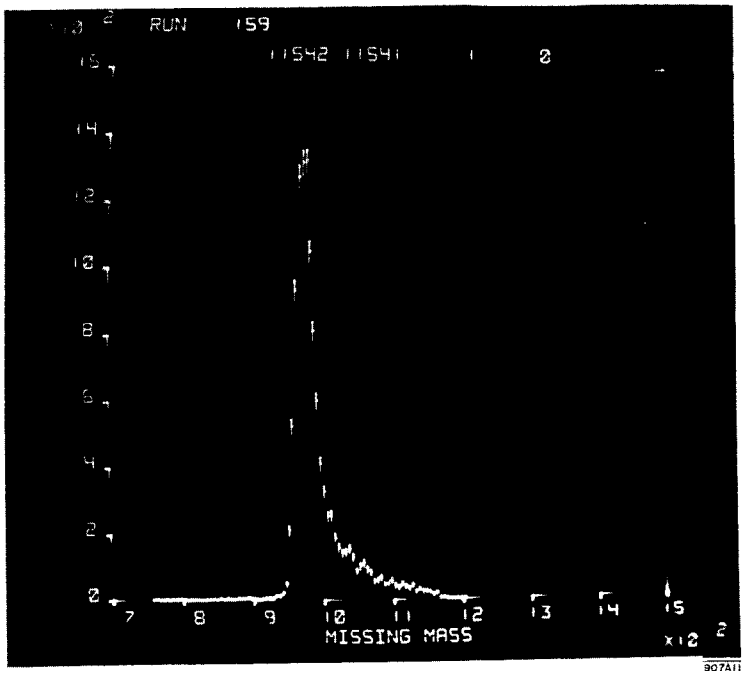

FIG. 12 --The missing mass spectrum evaluated from the "good events" in the p-θ plane of Fig. 11.

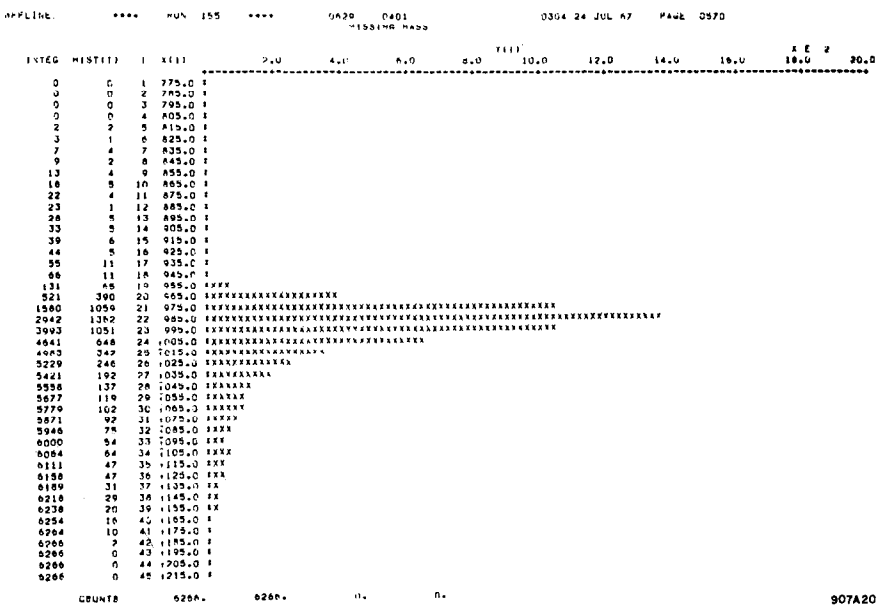

FIG. 13 --The scope displays may be alternatively output on a line printer. As an example, we show a typical missing mass spectrum.

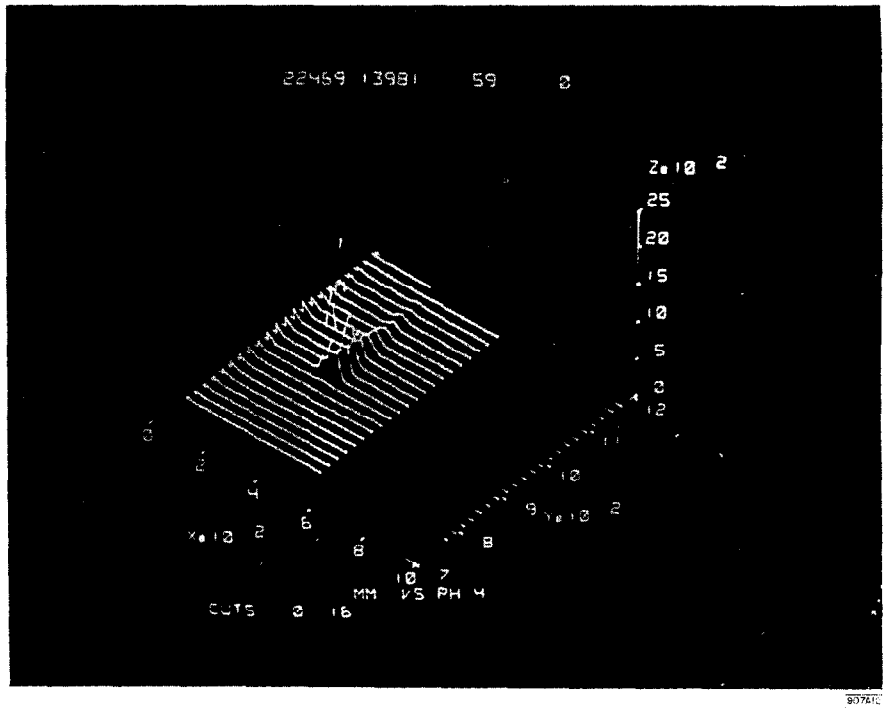

FIG. 14 --This 3-dimensional display has the total absorption shower counter pulse height (from Fig. 10) along the x-axis and the missing mass (from Fig. 12) along the y-axis. The elastically scattered electrons appear distinctly separated from the background events of lower pulse height.

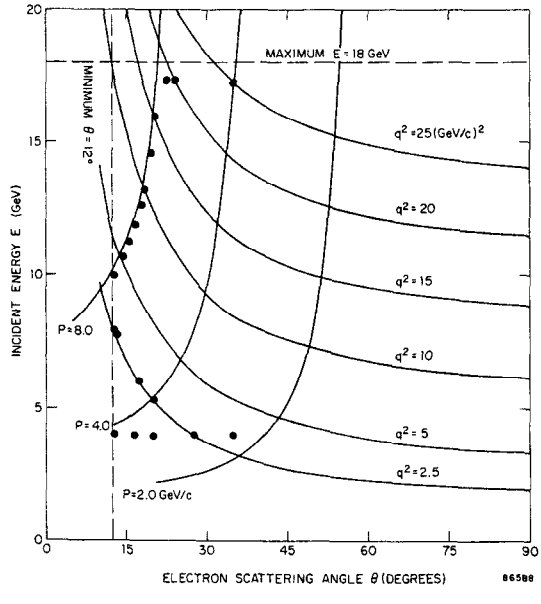

FIG. 15 --Lines of constant four-momentum transfer squared (q^2) are shown on a plot of incident electron energy and scattering angle. The points indicate the kinematic conditions of our present measurements.

$\Delta\Omega$ is the solid angle calculated from beam tracing tests of the spectrometer optics.

C is to allow for several corrections to the data.

The more important corrections applied in this analysis were:

1. Radiative corrections.

These have been applied for two contributions:

a. The Schwinger effect, in which radiation due to the elastic electron-proton scattering process has been calculated using the formula of Meister and Yennie.[3] We assume exponentiation of the "δ" factor, which results in a multiplicative correction factor of between 1.23 - 1.40 for our data.

b. Real bremsstrahlung due to material in the path of the electrons "before" and "after" the scattering process. For the target lengths used in this experiment, this correction was large, varying from 1.19 - 1.36.

2. Electronic and computer deadtimes.

The beam intensity was adjusted to reduce the effect of electronic and computer deadtimes to less than a few percent for most of the data runs. These deadtimes were accurately monitored during the runs. In general, the efficiency of the total absorption counter was assumed to be 1.000, although an allowance was made for runs in which a significant background contribution was present just above the pulse height requirement for this counter.

3. Event decoding.

Approximately 92% of the "good events" had unambiguous signals in the hodoscope arrays. Of the remaining 8%, approximately 5% were due to double tracks or uncertainties arising from inefficient counters in the hodoscopes. These could be recovered, and when put on the p-θ plane they reproduced the elastic peak distribution of the unambiguous events. The remaining 3% remain ambiguous at this time, but it is hoped that they will be understood with further analysis.

Our present estimates of the normalization and relative errors are shown in Table II. Some of the errors will presumably be reduced as better studies of the apparatus and further analysis of the data are accomplished.

Since in general we have only one measurement for each momentum transfer, we cannot exhibit Rosenbluth plots. In order to extract G_M from our present data we must make two assumptions:

1. the validity of the Rosenbluth relation

2. $G_E = G_M/\mu$.

TABLE II

The Correction Factor and Error Contributions for a Typical Cross Section Calculation

$$\frac{d\sigma}{d\Omega} = \frac{N_{pk}C}{N_e N_p \Delta\Omega}$$

Correction or Error (example)	Correction Factor C	Normalization Errors %	Relative Errors %
Current Monitor	--	0.0	1.5
Target Length	--	0.0	0.3
Target Density	--	1.5	0.0
θ Dispersion	--	0.25	0.0
Φ Acceptance	--	4.0	0.5
Scattering Angle	--	0.4	0.0
Primary Energy	--	1.5	0.0
Variation of Cross Section	0.997	0.0	0.0
Radiative Correction	1.297	3.0	1.0
Bremsstrahlung	1.330	1.0	0.0
Trigger Efficiency	1.010	0.0	0.0
Shower Counter Efficiency	1.000	0.0	0.0
Electronics Deadtime	1.010	0.0	0.3
Computer Deadtime	1.020	0.0	0.0
Tape Loss	1.005	0.0	0.0
Decoding Loss	1.080	3.0	0.4
Event Selection	1.000	1.0	0.5
TOTAL	1.942	6.4	2.0
Counting Statistics	--	--	variable

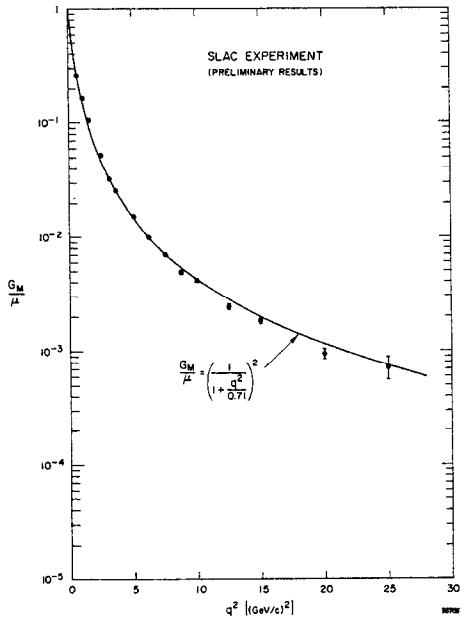

FIG. 16 --The SLAC values of G_M/μ are plotted against the square of the four momentum transfer (q^2). The curve is the best fit to the dipole model at lower energies.[5]

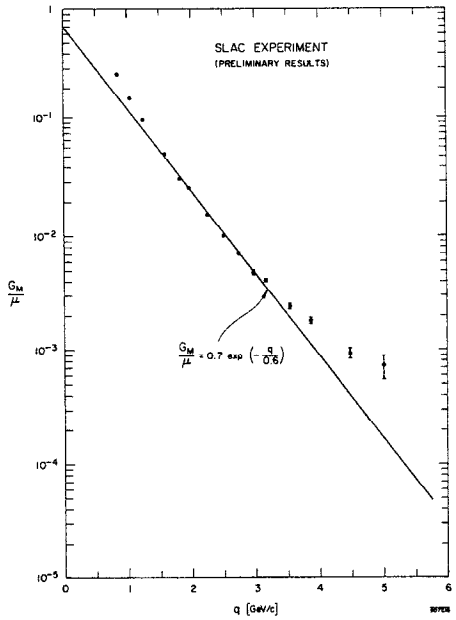

FIG. 17 --The SLAC data are compared to the Wu and Yang expression[6] for the asymptotic behavior of the form factors.

These assumptions have been verified at lower momentum transfers.[4] The factor G_M dominates in the Rosenbluth cross section for large momentum transfers, so that in this region assumption (2) need be only approximately true. For example, $G_E = 0$ would affect the values of G_M by less than $\sim 4\%$ at transfers above $5\,(\mathrm{GeV/c})^2$. Table III lists the values of the cross sections and, with the above assumptions, values of G_M/μ obtained in this preliminary analysis.

IV. COMPARISON OF RESULTS WITH THEORY

In Fig. 16, our values are shown plotted against q^2. The solid line is obtained from the dipole model

$$\frac{G_M}{\mu} = \left\{ \frac{1}{1 + \frac{q^2}{0.71}} \right\}^2 \qquad (2)$$

where the parameter $0.71\ (\mathrm{GeV/c})^2$ is obtained from a best fit to the lower energy data.[5] This model postulates two resonances of nearly equal mass near the mass of the ρ meson. There is no evidence that this is indeed so, and the only virtue of this model is the accuracy with which it fits the data. The lower energy data has already shown that fits utilizing the known vector mesons are unsatisfactory.[5]

There have been several attempts to link the proton-proton and electron-proton scattering data. Wu and Yang conjectured[6] that one could replace the transverse momentum transfer ($p_\perp$) in the Orear expression[7] for large angle p-p elastic scattering by $(q^2)^{1/2}$ and get an asymptotic expression for the form factors of the form

$$\frac{G_M}{\mu} \sim B \exp \left\{ - \frac{\left(q^2\right)^{\frac{1}{2}}}{0.6} \right\} \qquad (3)$$

The fit to our data is shown in Fig. 17 where B is taken as a constant. The lack of a fit at high q^2 may be, as Wu and Yang remark, an indication that B is a function of q^2. Also, it may be that we are not yet in the asymptotic region.

A recent model by Schopper[8] was fitted to the low energy e-p scattering essentially by two exponentials and his fit continues to be good when our data is added, as seen in Fig. 18. However, this model is not so good a fit to the proton data.

Allaby, et al.,[9] have recently obtained a rather spectacular fit to the proton data using exponentials of the form $\exp(-s \sin\theta/g)$, where g is a constant for each exponential. In the preceding paper by G. Weber, the data up to $10\ (\mathrm{GeV/c})^2$ were shown to be a good fit when $(s \sin\theta)$ is replaced by $(2\,q^2)$. In Fig. 19, we see that the fit is not so good for the high q^2 data.

Drell, et al., have explored[10] several models for asymptotic behavior, leading to the so-called fractional exponential models. The simplest of these has the form:

$$\frac{G_M}{\mu} = A \exp \left\{ - \left(\frac{q}{q_0} \right)^{\frac{1}{2}} \right\} \qquad (4)$$

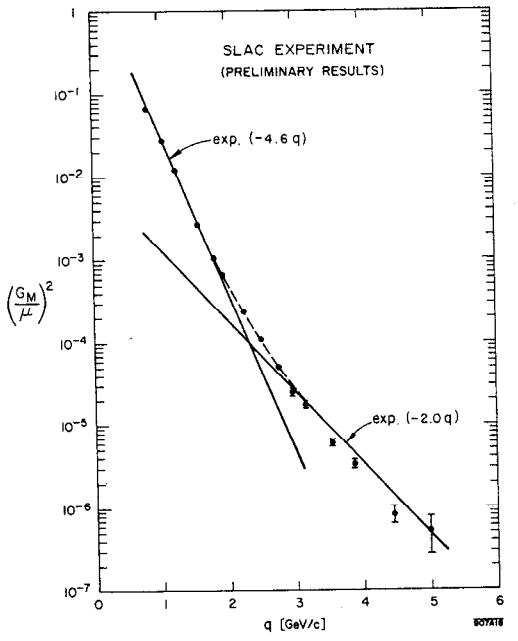

FIG. 18 --The SLAC data are in good agreement with a model due to Schopper[8].

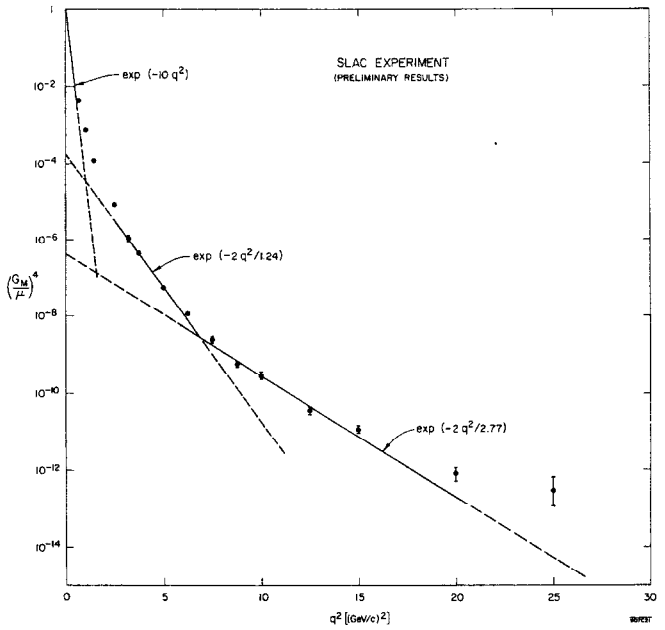

FIG. 19 --A recent fit by Allaby, et al.,[9] to the proton-proton elastic data is compared to the SLAC electron-proton data, as described in the text. The fit is not so good at high q^2 values.

where A and q_0 are constants. This form is compared to our data in Fig. 20, where the agreement is quite good. A smaller exponent of approximately 1/4 would be a better fit to the data at high q^2.

The present theoretical situation with regard to the form factors is not very satisfactory. No real understanding of the form factors is evident, and it is not yet clear whether the more restricted goal of linking e-p and p-p scattering can be accomplished in a convincing way. In this connection we would welcome further information on what variable in p-p scattering corresponds to the momentum transfer in e-p scattering. While the accuracy of G_M measurements for the proton may increase somewhat as time goes on, the range will not be greatly extended for some time to come.

Figure 21 is a compilation of world data[11] above 0.7 $(GeV/c)^2$, including the SLAC data of this paper. We have plotted the cross section ratio (σEXPT/σDIPOLE), which makes evident any disagreement with the dipole prediction. The previous logarithmic plots are not so sensitive to small discrepancies. Normalization errors (see Table II) in our values are not shown but we do not expect them to be greater than $\sim$ 6%. However, further analysis of our results is in progress, particularly in evaluating the radiative corrections which are somewhat larger in our case than in the data from other laboratories. There appears to be definite evidence in the world data for a significant deviation from the smooth dipole fit. This deviation is in a region accessible to SLAC, DESY, and CEA, so that very soon we should have good information in this region, and hopefully better agreement between the different laboratories.

As this is the first experimental paper from SLAC at this conference it would be appropriate for me to express the gratitude which all of us involved with SLAC feel towards the people who have built and now operate this new accelerator. We hope that the physics we can do will justify their magnificent efforts over the past several years.

Notes Added in Proof

1. The SLAC data presented in Fig. 21 and Table III of this paper are more recent data than those presented to the conference. An improved correction for bremsstrahlung straggling has reduced the cross sections previously reported.

2. The statement that three-pole fits based on the known vector mesons are unsatisfactory may be premature according to a preprint by V. Wataghin, "Nucleon Electromagnetic Form Factors and Vector Boson Resonances," (Submitted to Nuovo Cimento, August 1967).

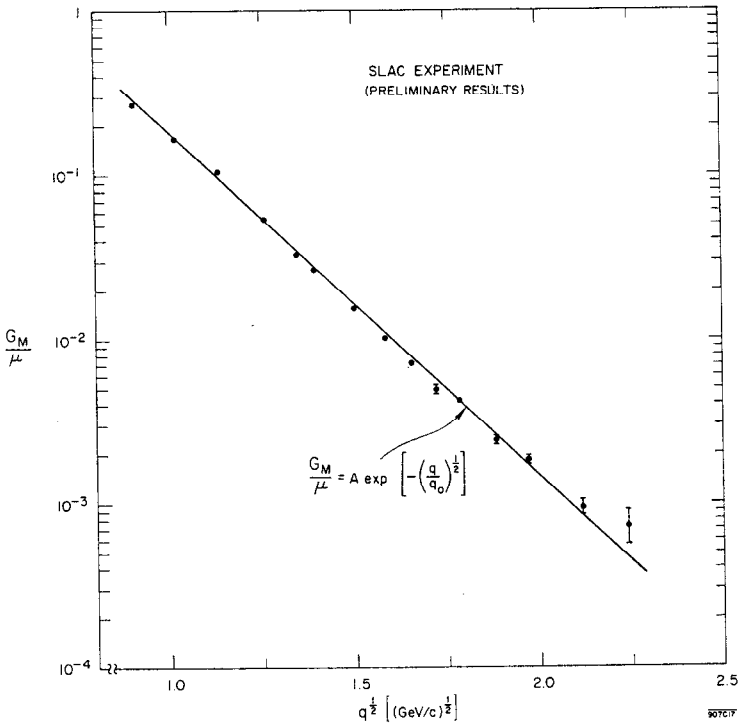

FIG. 20 --The SLAC data are compared with the simplest form of the fractional exponential model of Drell, et al.[10] A smaller exponent of approximately 1/4 would be a better fit to the data at high momentum transfers.

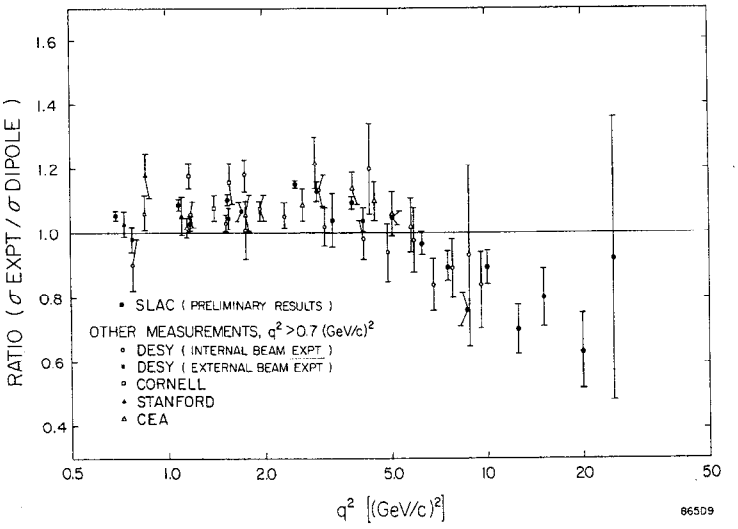

FIG. 21 --The world elastic electron-proton cross section data[11] for $q^2 > 0.7$ (GeV/c)^2 and the SLAC data are compared to the dipole model prediction. Normalization errors in the SLAC values are not shown, but these are not expected to be greater than ~6%. There appears to be definite evidence in the data for a significant deviation from the dipole fit.

TABLE III

SLAC Preliminary Electron-Proton Elastic Scattering Data

(These values have been calculated using the Rosenbluth equation and assuming $G_E = G_M/\mu$.)

q^2 $(GeV/c)^2$	INCIDENT ELECTRON ENERGY (GeV)	ELECTRON SCATTERING ANGLE (degree)	$\frac{d\sigma}{d\Omega}$ $(cm^2/ster)$	$\frac{G_M}{\mu}$
0.690	4.004	12.50	$(.3097 \pm .0036)\ 10^{-30}$	$.2640 \pm .0015$
1.091	3.998	16.25	$(.4897 \pm .0086)\ 10^{-31}$	$.1630 \pm .0014$
1.538	4.003	20.00	$(.997 \pm .016)\ 10^{-32}$	$.1053 \pm .0008$
2.505	7.905	12.61	$(.5102 \pm .0040)\ 10^{-32}$	$(.5245 \pm .0021)\ 10^{-1}$
2.609	7.909	12.92	$(.4255 \pm .0062)\ 10^{-32}$	$(.4998 \pm .0036)\ 10^{-1}$
2.533	6.035	17.21	$(.2296 \pm .0051)\ 10^{-32}$	$(.5098 \pm .0056)\ 10^{-1}$
2.476	5.294	19.75	$(.1801 \pm .0042)\ 10^{-32}$	$(.5285 \pm .0062)\ 10^{-1}$
2.444	4.004	27.50	$(.833 \pm .027)\ 10^{-33}$	$(.5398 \pm .0086)\ 10^{-1}$
3.270	4.002	35.00	$(.123 \pm .010)\ 10^{-33}$	$(.325 \pm .013)\ 10^{-1}$
3.770	10.000	12.47	$(.970 \pm .017)\ 10^{-33}$	$(.2644 \pm .0023)\ 10^{-1}$
5.082	10.702	14.00	$(.1913 \pm .0048)\ 10^{-33}$	$(.1538 \pm .0019)\ 10^{-1}$
5.000	10.001	15.00	$(.1772 \pm .0077)\ 10^{-33}$	$(.1600 \pm .0035)\ 10^{-1}$
6.276	11.349	15.10	$(.571 \pm .023)\ 10^{-34}$	$(.1022 \pm .0021)\ 10^{-1}$
7.512	12.000	16.08	$(.195 \pm .010)\ 10^{-34}$	$(.711 \pm .018)\ 10^{-2}$
8.766	12.700	16.86	$(.707 \pm .053)\ 10^{-35}$	$(.495 \pm .019)\ 10^{-2}$
9.992	13.320	17.62	$(.392 \pm .023)\ 10^{-35}$	$(.421 \pm .012)\ 10^{-2}$
12.49	14.657	18.78	$(.840 \pm .087)\ 10^{-36}$	$(.244 \pm .013)\ 10^{-2}$
15.02	16.008	19.72	$(.328 \pm .038)\ 10^{-36}$	$(.184 \pm .011)\ 10^{-2}$
20.03	17.806	22.90	$(.45 \pm .13)\ 10^{-37}$	$(.103 \pm .015)\ 10^{-2}$
20.00	17.314	24.04	$(.284 \pm .066)\ 10^{-37}$	$(.88 \pm .10)\ 10^{-3}$
25.03	17.314	35.09	$(.42 \pm .20)\ 10^{-38}$	$(.73 \pm .17)\ 10-3$

References

1. D. Yount, Nucl. Inst. and Meth. 52, 1 (1967).

2. L. Mo and C. Peck, Report No. SLAC-TN-65-29, (1965).

3. N. Meister and D. R. Yennie, Phys. Rev. 130, 1210 (1963).

4. H. J. Behrend, et al., Nuovo Cimento 48, 140 (1967).

5. M. Goitein, J. R. Dunning, and Richard Wilson, Phys. Rev. Letters 18, 1018 (1967).

6. T. T. Wu and C. N. Yang, Phys. Rev. 137, B708 (1965).

7. J. Orear, Phys. Rev. Letters 12, 112 (1964).

8. H. Schopper, CERN Internal Report 67-3 (1967).

9. J. V. Allaby, et al., CERN Internal Report 67-8 (1967).

10. S. D. Drell, A. C. Finn, and Michael H. Goldhaber, Phys. Rev. 157, 1402 (1967).

11. The world data compilation of results for $q^2 > 0.7$ $(GeV/c)^2$ have been taken from the following papers:

    Stanford: T. Janssens, R. Hofstadter, E. B. Hughes and M. R. Yearian, Phys. Rev. 142, 922 (1966);
    Cornell: K. Berkelman, et al., Phys. Rev. 130, 2061 (1963);
    CEA: M. Goitein, et al., Phys. Rev. Letters 18, 1016 (1967);
    DESY (internal beam experiment): H. J. Behrend, et al., Nuovo Cimento 48, 140 (1967); W. Albrecht, et al., Phys. Rev. Letters 17, 1192 (1966); W. Albrecht, et al., Phys. Rev. Letters 18, 1014 (1967);
    DESY (external beam experiment): W. Bartel, et al., Phys. Rev. Letters 17, 608 (1966); W. Bartel, et al., DESY Internal Report 67-18 (1967).

Discussion

R. Wilson, Harvard University

I would like to point out one thing which neither speaker mentioned. When you compare the data to the dipole fit as a ratio there are two "wiggles". There is a fall-off above about $4(GeV/c)^2$ which SLAC has confirmed. But in addition, the low energy data confirm a reduction below the line at about 0.25 $(GeV/c)^2$ which is there consistently in the Orsay, Stanford Mark III, DESY external beam, and CEA external beam data. These data agree to 2% with errors of 3 - 4% each, and are about 8% below the dipole fit.

R. G. Sachs, Argonne National Laboratory

I want to ask what may be a rather old-fashioned question. There was a time when we used to worry about the possibility that the form factor would level off as we go to a higher momentum transfer. In principle this would give us a measure of a significant constant: the wave-function renormalization constant for strong interactions. You did not consider this possibility in your discussion. Of course, if the so-called dipole fit is really so good then it is obvious that you have not yet gone to high enough momentum transfer to see it levelling off. On the other hand, your last plot shows that the dipole fit is not so good. The question is whether anyone has looked into the possibility of putting in a constant term plus something which decreases to see whether some of these wiggles might smooth out a bit?

G. Weber, DESY

We have tried only a small fraction of possibilities which one should consider. I think that, since there are finite errors, it is probably possible to introduce a core. I am not able to say how big it might be, but I am sure that you cannot exclude it.

V. P. Dzhelepov, Joint Institute for Nuclear Research, Dubna

I have a question for Dr. Taylor. What minimum cross section can you measure with your experiment and beam intensity?

R. E. Taylor, Stanford Linear Accelerator Center

The highest cross section was about 10^{-31} cm^2/sr and the lowest was about 2×10^{-39} cm^2/sr.

W. Jentschke, Session Chairman, DESY

What hopes do you have to go to even lower cross sections?

R. E. Taylor

There is supposed to be a factor of three to come in the electron current.

W. Jentschke

Could you state the lowest counting rate which you have had?

R. E. Taylor

The lowest cross section was the run in which we had 7 counts in 24 hours.

W. Jentschke

And your target-empty rate was ... ?

R. E. Taylor

We did not take an empty-target run at that point.